Regular Article

(*Z*)-2-(Benzo[*d*]thiazol-2-ylamino)-5-(substituted benzylidene)thiazol-4(5*H*)-one Derivatives as Novel Tyrosinase Inhibitors

Kyeong Ha Kang,[a,#] Bonggi Lee,[a,#] Sujin Son,[a,b] Hwi Young Yun,[a,b] Kyoung Mi Moon,[a] Hyoung Oh Jeong,[a] Dae Hyun Kim,[a,b] Eun Kyeong Lee,[a] Yeon Ja Choi,[a] Do Hyun Kim,[a,b] Pusoon Chun,[c] Hyung Ryong Moon,*[a,b] and Hae Young Chung*[a,b]

[a] *College of Pharmacy, Pusan National University; Busan 609–735, Republic of Korea: and* [b] *Molecular Inflammation Research Center for Ageing Intervention (MRCA), Pusan National University; Busan 609–735, Republic of Korea: and* [c] *College of Pharmacy, Inje University; Gimhae, Gyeongnam 621–749, Republic of Korea.*
Received April 2, 2015; accepted May 18, 2015

Inhibiting tyrosinase is an important goal to prevent melanin accumulation in skin and thereby to inhibit pigmentation disorders. Therefore, tyrosinase inhibitors are an attractive target in cosmetics and treatments for pigmentation disorders. However, only a few tyrosinase inhibitors are currently available because of their toxic effects to skin or lack of selectivity and stability. Here, we newly synthesized thirteen (*Z*)-2-(benzo[*d*]thiazol-2-ylamino)-5-(substituted benzylidene)thiazol-4(5*H*)-one derivatives and examined their effect on melanogenesis. Of these compounds, MHY2081 had the strongest inhibitory effect on tyrosinase without cytotoxicity in B16F10 melanoma cells. Consistently, melanogenesis was notably decreased by MHY2081 treatment. As an underlying mechanism, docking simulation showed that compared to kojic acid, a well-known competitive tyrosinase inhibitor which forms a hydrogen bond and aromatic interaction with tyrosinase, MHY2081 has stronger affinity with tyrosinase by forming three hydrogen bonds and a hydrophobic interaction with residues of tyrosinase. In parallel with this, Lineweaver–Burk plot analysis showed that MHY2081 is a strong competitive inhibitor of tyrosinase. In conclusion, MHY2081 may be a novel tyrosinase inhibitor for prevention and treatment of pigmentation disorders.

Key words skin; melanogenesis; tyrosinase inhibitor

The skin is a protective barrier against UV irradiation. Melanogenesis is an important function for skin to protect itself from damage.[1)] However, chronic and repeated exposures of UV lead to premature aging of the skin, which is called photoaging.[1)] In addition, melanin accumulation is able to increase pigmentation disorders such as melasma, freckles, and solar lentigo.[2,3)] Therefore, various compounds that prevent melanogenesis have been screened for cosmetics and preventing pigmentation disorders.

Melanogenesis is the process by which melanin is secreted by melanocytes located in the basal layer of the epidermis. Tyrosinase, a copper containing metalloenzyme, is one of the enzymes responsible for skin pigmentation in mammals.[4)] Tyrosinase catalyses two rate-limiting steps in melanogenesis: the hydroxylation of tyrosine to 3,4-dihydroxyphenylalanine (DOPA) and the oxidation of DOPA to DOPAquinone. Therefore, tyrosinase predominantly regulates melanin production[5)] and tyrosinase inhibitors are widely used for cosmetics and treatments for pigmentation disorders compared to other melanogenesis inhibitors. However, only a few tyrosinase inhibitors are currently used in cosmetics and medical products because of their cytotoxicity and lack of selectivity and stability.[6–8)]

Based on the structure of tyrosinase substrates L-tyrosin and L-DOPA, we synthesized a series of (*Z*)-2-(benzo[*d*]-thiazol-2-ylamino)-5-(substituted benzylidene)thiazol-4(5*H*)-one derivatives to screen for novel tyrosinase inhibitors. Here, our data show that MHY2081 is the strongest tyrosinase inhibitor among 13 synthesized compounds.

MATERIALS AND METHODS

Synthesis of Compounds (Chart 1)

N-(Benzo[*d*]thiazol-2-yl)-2-chloroacetamide (**14**)

To a stirred solution of 2-aminobenzothiazole (6.0 g, 39.95 mmol) in acetone (80 mL) was added a solution of chloroacetyl chloride (6.35 mL, 79.84 mmol) in acetone (20 mL) at 0°C and the reaction mixture was refluxed for 3 h. After cooling, the volatile solvent was removed under reduced pressure to give a residue, which was neutralized using aqueous sodium bicarbonate solution to pH 7. The precipitates generated were filtered and washed with water to give **14** (8.40 g, 92.8%) as a solid.

^{1}H-NMR (400 MHz, dimethyl sulfoxide (DMSO)-d_6) δ: 7.97 (d, 1H, J=7.6 Hz), 7.73 (d, 1H, J=8.4 Hz), 7.41 (t, 1H, J=8.0 Hz), 7.29 (t, 1H, J=8.0 Hz), 4.43 (s, 2H); ^{13}C-NMR (100 MHz, DMSO-d_6) δ: 166.6, 158.2, 149.1, 132.1, 126.9, 124.5, 122.5, 121.4, 43.2.

2-(Benzo[*d*]thiazol-2-ylamino)thiazol-4(5*H*)-one (**15**)

A suspension of **14** (4.0 g, 17.65 mmol) and ammonium thiocyanate (2.7 g, 35.47 mmol) in ethyl alcohol (40 mL) was refluxed for 4 h. After cooling, the reaction mixture was filtered and washed with cold EtOH to give **15** (3.01 g, 68.4%) as a solid.

^{1}H-NMR (400 MHz, DMSO-d_6) δ: 12.27 (s, 1H), 7.93 (d, 1H, J=8.0 Hz), 7.76 (d, 1H, J=8.0 Hz), 7.42 (t, 1H, J=8.0 Hz), 7.30 (t, 1H, J=8.0 Hz), 4.03 (s, 2H); ^{13}C-NMR (100 MHz, DMSO-d_6) δ: 175.0, 169.6, 166.8, 151.5, 133.7, 127.0, 124.9, 122.6, 122.0, 35.9.

General Procedure of (*Z*)-2-(Benzo[*d*]thiazol-2-ylamino)-5-(substituted benzylidene)thiazol-4(5*H*)-one Analogs (Com-

[#] These authors contributed equally to this work.

* To whom correspondence should be addressed. e-mail: mhr108@pusan.ac.kr; hyjung@pusan.ac.kr

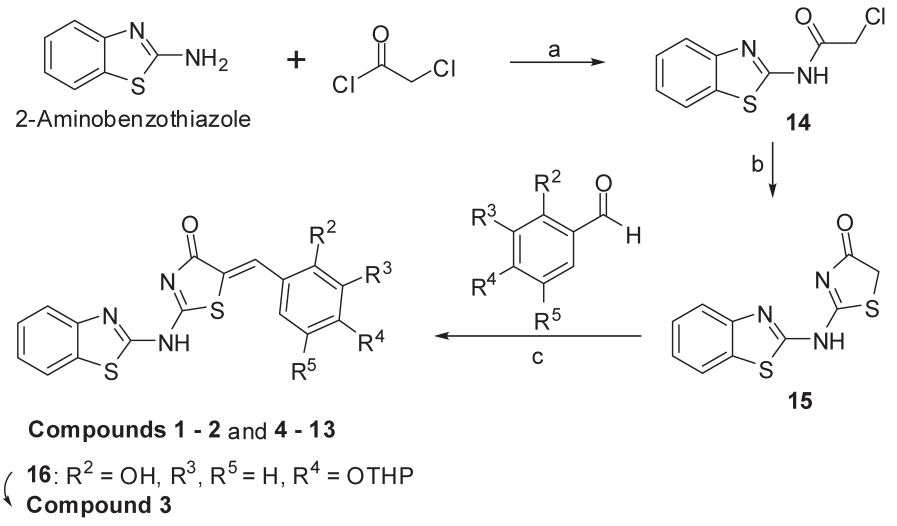

Reagents and conditions: (a) acetone, reflux, 3 h, 92.8%; (b) NH_4SCN, EtOH, reflux, 4 h, 68.4%; (c) NaOAc, AcOH, reflux, 10–35 h for **1**–**2** and **4**–**13**; piperidine, EtOH, reflux, 10 h for **16**; (d) 2 N-HCl, 1,4-dioxane, DMF, rt, overnight and then 50°C, 2 d for **3** (MHY2081).

Chart 1. Synthetic Scheme for Compounds **1**–**13**

pounds **1**–**2** and **4**–**13**)

A suspension of **15** (80 mg, 0.32 mmol), a variety of substituted benzaldehyde (1.1 eq.), and NaOAc (3.0 eq.) in acetic acid (1.0 mL) was refluxed for 10–35 h. After cooling, water was added and the precipitates generated were filtered and washed with water or MeOH/H_2O (8 : 1–1 : 2) to give compounds **1**–**2** and **4**–**13** as solids.

(*Z*)-2-(Benzo[*d*]thiazol-2-ylamino)-5-(4-hydroxybenzylidene)thiazol-4(5*H*)-one (**1**)

Reaction time, 10 h; yield, 66.5%; yellow solid; ^{1}H-NMR (400 MHz, DMSO-d_6) δ: 12.76 (br s, 1H, NH), 10.35 (s, 1H, OH), 7.96 (d, 1H, J=7.6 Hz, 4′-H), 7.91 (d, 1H, J=8.4 Hz, 7′-H), 7.66 (s, 1H, vinylic H), 7.53 (d, 2H, J=7.6 Hz, 2″-H, 6″-H), 7.46 (t, 1H, J=8.0 Hz, 5′-H), 7.33 (t, 1H, J=7.6 Hz, 6′-H), 6.93 (d, 2H, J=7.6 Hz, 3″-H, 5″-H); ^{13}C-NMR (100 MHz, DMSO-d_6) δ: 169.0, 167.9, 160.7, 159.6, 151.5, 134.0, 133.8, 133.4, 127.1, 125.1, 124.8, 122.7, 122.5, 120.3, 117.1; high resolution (HR)-MS-electrospray ionization (ESI) m/z $C_{17}H_{10}N_3O_2S_2$ $(M-H)^-$ Calcd 352.0214, obsd 352.0226.

(*Z*)-2-(Benzo[*d*]thiazol-2-ylamino)-5-(3,4-dihydroxybenzylidene)thiazol-4(5*H*)-one (**2**)

Reaction time, 22 h; yield, 89.4%; greenish yellow solid; ^{1}H-NMR (400 MHz, DMSO-d_6) δ: 12.74 (brs, 1H, NH), 9.89 (brs, 1H, OH), 9.56 (brs, 1H, OH), 7.92 (d, 1H, J=7.6 Hz, 4′-H), 7.91 (d, 1H, J=7.6 Hz, 7′-H), 7.57 (s, 1H, vinylic H), 7.44 (t, 1H, J=7.6 Hz, 5′-H), 7.30 (t, 1H, J=7.6 Hz, 6′-H), 7.11 (s, 1H, 2″-H), 7.02 (d, 1H, J=7.2 Hz, 6″-H), 6.89 (d, 1H, J=7.2 Hz, 5″-H); ^{13}C-NMR (100 MHz, DMSO-d_6) δ: 169.0, 168.0, 160.0, 151.6, 149.5, 146.6, 134.5, 133.9, 127.1, 125.3, 125.1, 125.0, 122.7, 122.4, 120.1, 117.3, 117.0; HR-MS-ESI m/z $C_{17}H_{10}N_3O_3S_2$ $(M-H)^-$ Calcd 368.0164, obsd 368.0169.

(*Z*)-2-(Benzo[*d*]thiazol-2-ylamino)-5-(4-hydroxy-3-methoxybenzylidene)thiazol-4(5*H*)-one (**4**)

Reaction time, 17 h; yield, 73.6%; brown solid; ^{1}H-NMR (400 MHz, DMSO-d_6) δ: 12.47 (brs, 1H, NH), 10.00 (s, 1H, OH), 7.96 (d, 1H, J=7.6 Hz, 4′-H), 7.84 (d, 1H, J=8.0 Hz, 7′-H), 7.67 (s, 1H, vinylic H), 7.46 (t, 1H, J=8.0 Hz, 5′-H), 7.33 (t, 1H, J=8.0 Hz, 6′-H), 7.27 (s, 1H, 2″-H), 7.16 (d, 1H, J=8.0 Hz, 6″-H), 6.95 (d, 1H, J=8.4 Hz, 5″-H), 3.85 (s, 3H, OCH_3); ^{13}C-NMR (100 MHz, DMSO-d_6) δ: 169.0, 167.9, 159.8, 151.5, 150.2, 148.7, 134.3, 133.8, 127.2, 125.4, 125.1, 122.8, 122.3, 120.7, 116.9, 115.1, 56.2; HR-MS-ESI m/z $C_{18}H_{12}N_3O_3S_2$ $(M-H)^-$ Calcd 382.0320, obsd 382.0333.

(*Z*)-2-(Benzo[*d*]thiazol-2-ylamino)-5-(3-ethoxy-4-hydroxybbenzylidene)thiazol-4(5*H*)-one (**5**)

Reaction time, 14 h; yield, 95.1%; yellow solid; ^{1}H-NMR (400 MHz, DMSO-d_6) δ: 9.91 (s, 1H, OH), 7.93 (d, 1H, J=8.0 Hz, 4′-H), 7.79 (d, 1H, J=7.6 Hz, 7′-H), 7.64 (s, 1H, vinylic H), 7.44 (t, 1H, J=7.6 Hz, 5′-H), 7.30 (t, 1H, J=7.6 Hz, 6′-H), 7.22 (s, 1H, 2″-H), 7.13 (d, 1H, J=8.0 Hz, 6″-H), 6.94 (d, 1H, J=8.0 Hz, 5″-H), 4.10 (q, 2H, J=6.8 Hz, OCH_2), 1.38 (t, 3H, J=6.8 Hz, CH_2CH_3); ^{13}C-NMR (100 MHz, DMSO-d_6) δ: 169.0, 167.9, 159.8, 151.5, 150.4, 147.7, 134.3, 133.8, 127.1, 125.3, 125.0, 122.7, 122.1, 120.6, 117.0, 116.0, 64.5, 15.3; HR-MS-ESI m/z $C_{19}H_{14}N_3O_3S_2$ $(M-H)^-$ Calcd 396.0477, obsd 396.0490.

(*Z*)-2-(Benzo[*d*]thiazol-2-ylamino)-5-(3-hydroxy-4-methoxybenzylidene)thiazol-4(5*H*)-one (**6**)

Reaction time, 15 h; yield, 98.7%; yellow solid; ^{1}H-NMR (400 MHz, DMSO-d_6) δ: 12.77 (brs, 1H, NH), 9.58 (s, 1H, OH), 7.96 (d, 1H, J=7.6 Hz, 4′-H), 7.89 (d, 1H, J=8.0 Hz, 7′-H), 7.60 (s, 1H, vinylic H), 7.46 (t, 1H, J=8.0 Hz, 5′-H), 7.33 (t, 1H, J=7.6 Hz, 6′-H), 7.14 (d, 1H, J=8.4 Hz, 6″-H), 7.11 (s, 1H, 2″-H), 7.07 (d, 1H, J=8.4 Hz, 5″-H), 3.81 (s, 3H, OCH_3); ^{13}C-NMR (100 MHz, DMSO-d_6) δ: 169.0, 167.9, 159.6, 151.5, 150.8, 147.6, 134.0, 133.9, 127.2, 126.6, 125.1, 124.6, 122.7, 122.4, 121.3, 116.8, 113.1, 56.4; HR-MS-ESI m/z $C_{18}H_{12}N_3O_3S_2$ $(M-H)^-$ Calcd 382.0320, obsd 382.0334.

(*Z*)-2-(Benzo[*d*]thiazol-2-ylamino)-5-(4-methoxybenzylidene)thiazol-4(5*H*)-one (**7**)

Reaction time, 14 h; yield, 82.9%; yellow solid; ^{1}H-NMR (400 MHz, DMSO-d_6) δ: 7.94 (d, 1H, J=7.6 Hz, 4′-H), 7.89 (d, 1H, J=7.6 Hz, 7′-H), 7.68 (s, 1H, vinylic H), 7.61 (d, 2H, J=8.0 Hz, 2″-H, 6″-H), 7.45 (t, 1H, J=7.6 Hz, 5′-H), 7.32 (t, 1H, J=7.6 Hz, 6′-H), 7.09 (d, 2H, J=8.0 Hz, 3″-H, 5″-H), 3.81 (s, 3H, OCH_3); ^{13}C-NMR (100 MHz, DMSO-d_6) δ: 168.9, 167.9, 161.7, 159.4, 151.5, 133.9, 133.4, 133.0, 127.1, 126.4, 125.1, 122.7, 122.4, 121.6, 115.6, 56.1; HR-MS-ESI m/z $C_{18}H_{12}N_3O_2S_2$ $(M-H)^-$ Calcd 366.0371, obsd 366.0383.

(*Z*)-2-(Benzo[*d*]thiazol-2-ylamino)-5-(3,4-dimethoxybenzyl-

idene)thiazol-4(5*H*)-one (**8**)

Reaction time, 15 h; yield, 85.5%; yellow solid; ^{1}H-NMR (400 MHz, DMSO-d_6) δ: 7.95 (d, 1H, J=7.6 Hz, 4′-H), 7.81 (d, 1H, J=8.0 Hz, 7′-H), 7.69 (s, 1H, vinylic H), 7.45 (t, 1H, J=8.0 Hz, 5′-H), 7.32 (t, 1H, J=8.0 Hz, 6′-H), 7.27–7.25 (m, 2H, 2″-H, 6″-H), 7.13 (d, 1H, J=8.0 Hz, 5″-H), 3.83 (s, 3H, OCH_3), 3.80 (s, 3H, OCH_3); ^{13}C-NMR (100 MHz, DMSO-d_6) δ: 169.0, 167.8, 159.6, 151.5, 151.5, 149.6, 133.8, 133.8, 127.2, 126.6, 125.1, 124.7, 122.8, 122.2, 122.0, 114.2, 112.8, 56.4, 56.1; HR-MS-ESI m/z $C_{19}H_{14}N_3O_3S_2$ $(M-H)^-$ Calcd 396.0477, obsd 396.0490.

(*Z*)-2-(Benzo[*d*]thiazol-2-ylamino)-5-(2,4-dimethoxybenzylidene)thiazol-4(5*H*)-one (**9**)

Reaction time, 17 h; yield, 92.2%; yellow solid; ^{1}H-NMR (400 MHz, DMSO-d_6) δ: 7.93 (d, 1H, J=7.6 Hz, 4′-H), 7.87–7.81 (m, 2H, vinylic H, 7′-H), 7.44 (d, 1H, J=8.8 Hz, 6″-H), 7.43 (t, 1H, J=7.2 Hz, 5′-H), 7.30 (t, 1H, J=7.6 Hz, 6′-H), 6.70 (dd, 1H, J=2.0, 8.8 Hz, 5″-H), 6.63 (d, 1H, J=2.0 Hz, 3″-H), 3.86 (s, 3H, OCH_3), 3.80 (s, 3H, OCH_3); ^{13}C-NMR (100 MHz, DMSO-d_6) δ: 169.0, 168.0, 163.8, 160.5, 159.9, 151.6, 133.8, 131.3, 128.1, 127.1, 125.0, 122.7, 122.3, 121.1, 115.2, 107.2, 99.3, 56.6, 56.3; HR-MS-ESI m/z $C_{19}H_{14}N_3O_3S_2$ $(M-H)^-$ Calcd 396.0477, obsd 396.0490.

(*Z*)-2-(Benzo[*d*]thiazol-2-ylamino)-5-(3,4,5-trimethoxybenzylidene)thiazol-4(5*H*)-one (**10**)

Reaction time, 17 h; yield, 98.2%; yellow solid; ^{1}H-NMR (400 MHz, DMSO-d_6) δ: 12.03 (brs, 1H, NH), 7.96 (d, 1H, J=8.0 Hz, 4′-H), 7.75 (d, 1H, J=8.0 Hz, 7′-H), 7.69 (s, 1H, vinylic H), 7.46 (t, 1H, J=7.6 Hz, 5′-H), 7.33 (t, 1H, J=7.6 Hz, 6′-H), 7.01 (s, 2H, 2″-H, 6″-H), 3.86 (s, 6H, 2×OCH_3), 3.72 (s, 3H, 4″-OCH_3); ^{13}C-NMR (100 MHz, DMSO-d_6) δ: 169.0, 167.7, 159.7, 153.9, 151.3, 140.0, 133.8, 133.7, 129.5, 127.3, 125.1, 124.2, 122.8, 122.2, 108.5, 60.9, 56.6; HR-MS-ESI m/z $C_{20}H_{16}N_3O_4S_2$ $(M-H)^-$ Calcd 426.0582, obsd 426.0591.

(*Z*)-2-(Benzo[*d*]thiazol-2-ylamino)-5-(4-hydroxy-3,5-dimethoxybenzylidene)thiazol-4(5*H*)-one (**11**)

Reaction time, 15 h; yield, 74.0%; yellow solid; ^{1}H-NMR (400 MHz, DMSO-d_6) δ: 12.74 (brs, 1H, NH), 9.39 (s, 1H, OH), 7.95 (d, 1H, J=8.0 Hz, 4′-H), 7.75 (d, 1H, J=7.6 Hz, 7′-H), 7.67 (s, 1H, vinylic H), 7.45 (t, 1H, J=7.6 Hz, 5′-H), 7.32 (t, 1H, J=7.6 Hz, 6′-H), 7.00 (s, 2H, 2″-H, 6″-H), 3.85 (s, 6H, 2×OCH_3); ^{13}C-NMR (100 MHz, DMSO-d_6) δ: 169.1, 167.8, 159.9, 151.4, 148.9, 139.3, 134.5, 133.8, 127.3, 125.1, 124.2, 122.8, 122.1, 121.2, 109.0, 56.7; HR-MS-ESI m/z $C_{19}H_{14}N_3O_4S_2$ $(M-H)^-$ Calcd 412.0426, obsd 412.0438.

(*Z*)-2-(Benzo[*d*]thiazol-2-ylamino)-5-(3-bromo-4-hydroxybenzylidene)thiazol-4(5*H*)-one (**12**)

Reaction time, 16 h; yield, 87.7%; brown solid; ^{1}H-NMR (400 MHz, DMSO-d_6) δ: 11.17 (brs, 1H, OH), 7.92 (d, 1H, J=7.2 Hz, 4′-H), 7.85–7.80 (m, 2H, 7′-H, 2″-H), 7.61 (s, 1H, vinylic H), 7.49 (d, 1H, J=8.0 Hz, 6″-H), 7.43 (t, 1H, J=7.2 Hz, 5′-H), 7.30 (t, 1H, J=7.2 Hz, 6′-H), 7.10 (d, 1H, J=8.0 Hz, 5″-H); ^{13}C-NMR (100 MHz, DMSO-d_6) δ: 168.9, 167.7, 159.3, 156.9, 151.4, 136.3, 133.8, 132.3, 131.4, 127.1, 126.6, 125.0, 122.7, 122.3, 117.6, 110.9; HR-MS-ESI m/z $C_{17}H_9BrN_3O_2S_2$ $(M-H)^-$ Calcd 429.9320, obsd 429.9323.

(*Z*)-2-(Benzo[*d*]thiazol-2-ylamino)-5-(3,5-dibromo-4-hydroxybenzylidene)thiazol-4(5*H*)-one (**13**)

Reaction time, 15 h; yield, 93.0%; yellow solid; ^{1}H-NMR (400 MHz, DMSO-d_6) δ: 7.96 (d, 1H, J=8.0 Hz, 4′-H), 7.83 (s, 2H, 2″-H, 6″-H), 7.78 (brd, 1H, J=7.6 Hz, 7′-H), 7.61 (s, 1H, vinylic H), 7.46 (t, 1H, J=8.0 Hz, 5′-H), 7.33 (t, 1H, J=8.0 Hz, 6′-H); ^{13}C-NMR (100 MHz, DMSO-d_6) δ: 168.9, 167.5, 158.9, 153.3, 151.3, 134.7, 133.9, 130.7, 128.3, 127.3, 125.2, 124.3, 122.8, 122.2, 113.0; HR-MS-ESI m/z $C_{17}H_8Br_2N_3O_2S_2$ $(M-H)^-$ Calcd 507.8425, obsd 507.8438.

Synthetic Procedure of (*Z*)-2-(Benzo[*d*]thiazol-2-ylamino)-5-(2,4-dihydroxybenzylidene)thiazol-4(5*H*)-one (**3**, MHY2081)

A solution of **15** (130 mg, 0.52 mmol) and 2-hydroxy-4-(tetrahydro-2*H*-pyran-2-yloxy)benzaldehyde (127.5 mg, 0.57 mmol) in EtOH (2.5 mL) was refluxed in the presence of piperidine (0.02 mL, 0.20 mmol) for 10 h. After cooling, water was added and the precipitates was filtered and washed with H_2O/MeOH (1/1) to give **16** (140 mg) as a crude solid, which was used for the next step without further purification. To a solution of **16** (140 mg) in 1,4-dioxane (0.7 mL) and DMF (0.5 mL) was added 2 N-HCl solution (0.7 mL) at room temperature and the reaction mixture was stirred at the same temperature overnight and heated at 50°C for 2 d. After cooling, water was added and the precipitates generated were filtered and washed with a small amount of MeOH to give **3** (MHY2081, 100.3 mg, 52.1% from **15**) as a solid.

Yellow solid; ^{1}H-NMR (500 MHz, DMSO-d_6) δ: 12.60 (br s, 1H, NH), 10.50 (brs, 1H, 2″-OH), 10.23 (brs, 1H, 4″-OH), 7.98 (s, 1H, vinylic H), 7.92 (d, 1H, J=7.5 Hz, 4′-H), 7.84 (brd, 1H, J=7.5 Hz, 7′-H), 7.43 (t, 1H, J=7.5 Hz, 5′-H), 7.35 (d, 1H, J=8.5 Hz, 6″-H), 7.30 (t, 1H, J=7.5 Hz, 6′-H), 6.47 (d, 1H, J=8.5 Hz, 5″-H), 6.45 (s, 1H, 3″-H); ^{13}C-NMR (100 MHz, DMSO-d_6) δ: 169.0, 168.2, 163.0, 162.5, 160.2, 151.6, 133.8, 131.1, 129.2, 127.0, 124.9, 122.6, 122.3, 118.2, 112.7, 109.1, 103.3; HR-MS-ESI m/z $C_{17}H_{10}N_3O_3S_2$ $(M-H)^-$ Calcd 368.0164, obsd 368.0179 (Supplementary Fig. 2).

Docking Simulation of Tyrosinase and MHY2081 Because of automated docking capability, AutoDock4.2 was used for the *in silico* protein–ligand docking simulation. The 3D structure of tyrosinase was used in the crystal structure of *Agaricus bisporus* (PDB ID: 2Y9X). As a docking pocket, predefined binding site of tyrosine was used. Docking simulations were performed between tyrosinase and MHY2081 or kojic acid. To prepare compounds for docking simulation, (1) 2D structures were converted into 3D structures, (2) charges were calculated, and (3) hydrogen atoms were added using the ChemOffice program (http://www.cambridgesoft.com). The prediction of possible hydrogen bonding residues between compounds and tyrosinase and generation of pharmacophores were analyzed with LigandScout 3.0 program.

Tyrosinase Activity Assay Using Mushroom Tyrosinase Tyrosinase activity was measured using commercially available mushroom tyrosinase. Twenty microliters of mushroom tyrosinase (1000 U) were added to a 96-well microplate (Nunc, Denmark) in 200 μL assay buffer containing 1 mM L-tyrosine solution and 50 mM phosphate buffer (pH 6.5). Various concentrations of MHY2081 or kojic acid were added to the microplate. After incubating the plate at 25°C for 30 min, the dopachrome production was measured using a microplate reader (Berthold, Bad Wildbad, Germany) at 492 nm. Based on this experiment, log–linear curves with their equations were obtained to calculate IC_{50} values, the concentration at which the *Y*-axis equaled to 50% inhibition of tyrosinase activity.

Kinetic Analysis of Tyrosinase Inhibition by MHY2081 Reaction mixture was prepared in a 96 well plate, in which

20 μL of L-tyrosine as a tyrosinase substrate, 10 μL of an aqueous mushroom tyrosinase solution (1000 U), and 50 mM potassium phosphate buffer (pH 6.5) were included. The initial rate of dopachrome formation from the reaction mixture was determined using a microplate reader (the increase in absorbance at 492 nm per min). The inhibitory kinetics of MHY2081 to tyrosinase was analyzed using Lineweaver–Burk plots. The Michaelis constant (K_m) and maximal velocity (V_{max}) of tyrosinase activity were determined by using Lineweaver–Burk plots with various concentrations of L-tyrosine substrate.

Cell Culture B16F10 murine melanoma cells were purchased from the Korea Cell Line Band. These cells were cultured in Dulbecco's modified Eagle's medium (DMEM) supplemented with 5% fetal bovine serum (FBS) and 1% penicillin streptomycin at 37°C in a humidified 95% air/5% CO_2 atmosphere. For experiments, the cells were seeded in 6-well plates and MHY2081, kojic acid, or α-melanocyte-stimulating hormone (α-MSH) was treated for 48 h when the cells were grown to 70–80%.

Cell Viability Assay 3-[4,5-Dimethylthiazol-2-yl]-3,5-diphenyltetrazolium bromide (MTT) assay was performed to examine cytototoxic effect of MHY2081. B16F10 melanoma

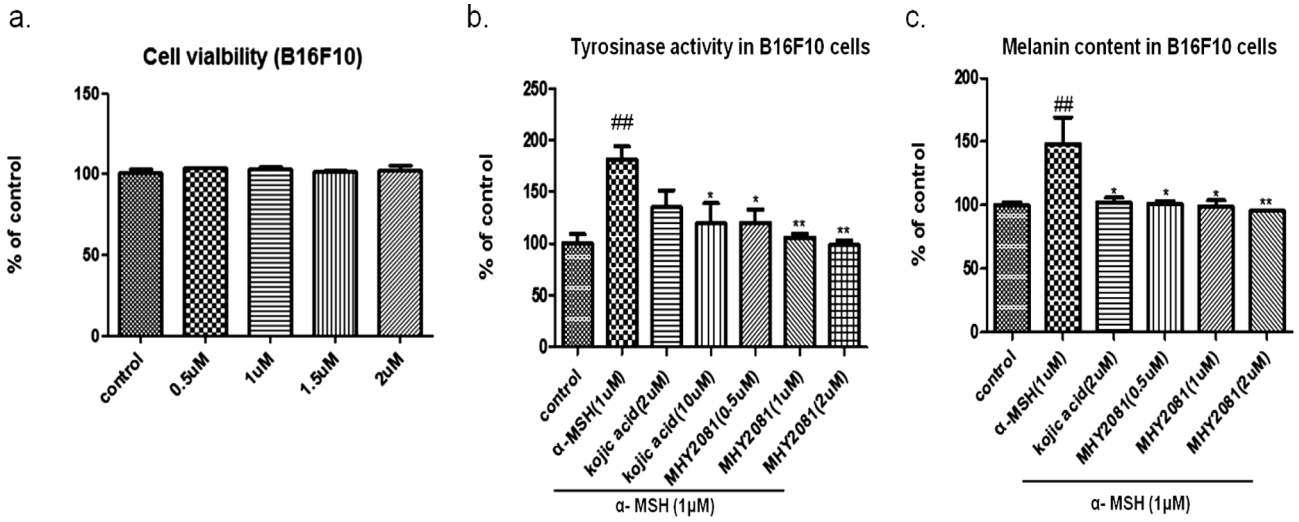

Fig. 1. The Inhibitory Effects of MHY2081 on Tyrosinase and Melanin Accumulation

(a) B16F10 melanoma cells were treated with various concentrations of MHY2081 for 48 h and then MTT assay was performed (n=3/group). Data are expressed as the percent of cell viability compared to a non-treated group. (b) Tyrosinase activity in B16F10 cells treated with MHY2081. B16F10 melanoma cells were pre-treated with MHY2081 or kojic acid for 2h and then the cells were treated with α-MSH (1 μM) for 48 h to stimulate melanogenesis (n=4/group). (c) B16F10 melanoma cells were pre-treated with MHY2081 or kojic acid for 2h and the cells were stimulated with α-MSH (1 μM) for 48 h. Melanin concentrations were determined using a microplate reader (n=4/group). The data are expressed as a mean±S.E.M. (n=4). *p<0.05 and **p<0.01 compared to the α-MSH-treated control group. $^{\#\#}p$<0.01 compared to the control group without α-MSH treatment.

Table 1. Substitution Pattern of the Substituted (*Z*)-2-(Benzo[*d*]thiazol-2-ylamino)-5-(substituted benzylidene)thiazol-4(5*H*)-one Derivatives

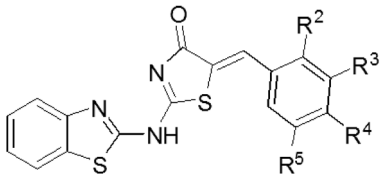

Compound	MHY	R^2	R^3	R^4	R^5	Tyrosinase inhibition (%)
1	1887	H	H	OH	H	8.756±0.56
2	1886	H	OH	OH	H	6.580±5.03
3	2081	OH	H	OH	H	96.82±2.85
4	2079	H	OMe	OH	H	NI
5	1885	H	OEt	OH	H	7.983±3.46
6	1880	H	OH	OMe	H	5.771±2.64
7	1883	H	H	OMe	H	NI
8	1881	H	OMe	OMe	H	NI
9	1888	OMe	H	OMe	H	NI
10	1942	H	OMe	OMe	OMe	NI
11	1884	H	OMe	OH	OMe	33.17±2.23
12	1879	H	Br	OH	Br	3.591±1.14
13	1882	H	Br	OH	Br	3.591±1.14

Tyrosinase inhibition was measured using mushroom tyrosinase and L-tyrosine as the substrate. Results are expressed as percentage of control and each value represents the mean±S.E.M. Repeated experiments showed the similar results. NI represents no inhibition.

Table 2. IC_{50} Values of Kojic Acid and MHY2081

Compound	MHY	Concentration (μM)	Tyrosinase inhibition (%)	IC_{50} (μM)
3	2081	0.2	24%	1.80±2.53
		2.5	57%	
		10	70%	
Kojic acid		5	21%	16.6±2.3
		10	33%	
		20	58%	

IC_{50} represents 50% inhibitory concentration.

cells were seeded into 96-well cell culture plates. After 24 h, the cells were exposed to MHY2081 at various concentrations for 48 h at 37°C under an atmosphere of 5% CO_2. MTT reagent (1 mg/mL in phosphate buffered saline) was added to each well and incubated for 2 h. Afterward, the media was removed, and the formazan crystals were dissolved in DMSO. Absorbance was measured at 560 nm. Cell viability was evaluated as the relative absorbance of the control group.

Determination of Melanin Level in B16F10 Melanoma Cells Cellular melanin content was measured based on the previously described method with a slight modification.[9] B16F10 melanoma cells were seeded in 6-well dishes and al-

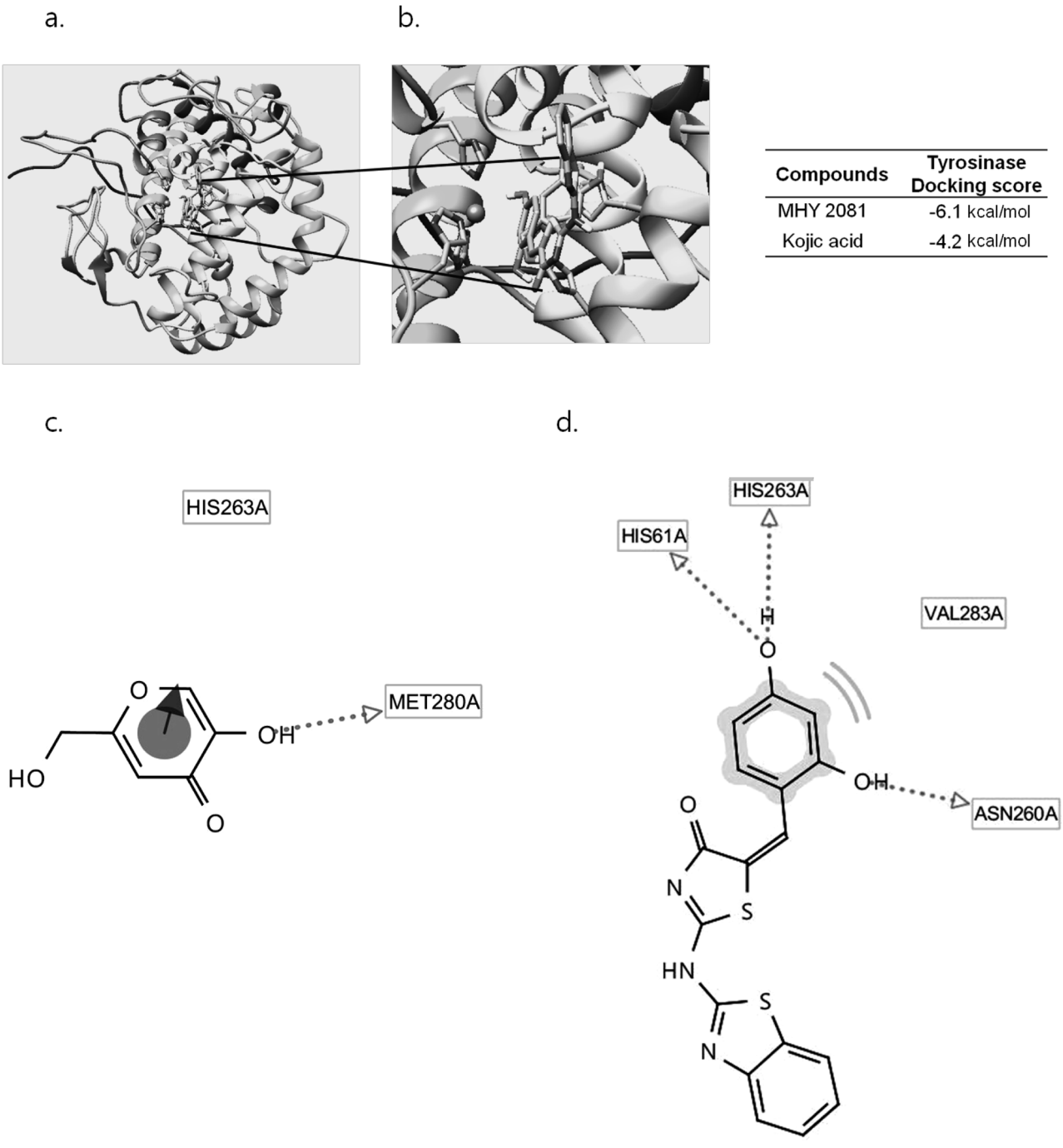

Fig. 2. MHY2081 Can Directly Bind to Tyrosinase

(a–d) Computational structure prediction for docking simulation between mushroom tyrosinase and MHY2081. (a) Predicted 3D structure of mushroom tyrosinase. The black lines indicate the binding site for MHY2081. (b) Magnified image of the binding site of MHY2081 in tyrosinase and a small table shows predicted binding affinity of MHY2081 and kojic acid with tyrosinase. The binding sites of (c) kojic acid and (d) MHY2081 with tyrosinase are shown.

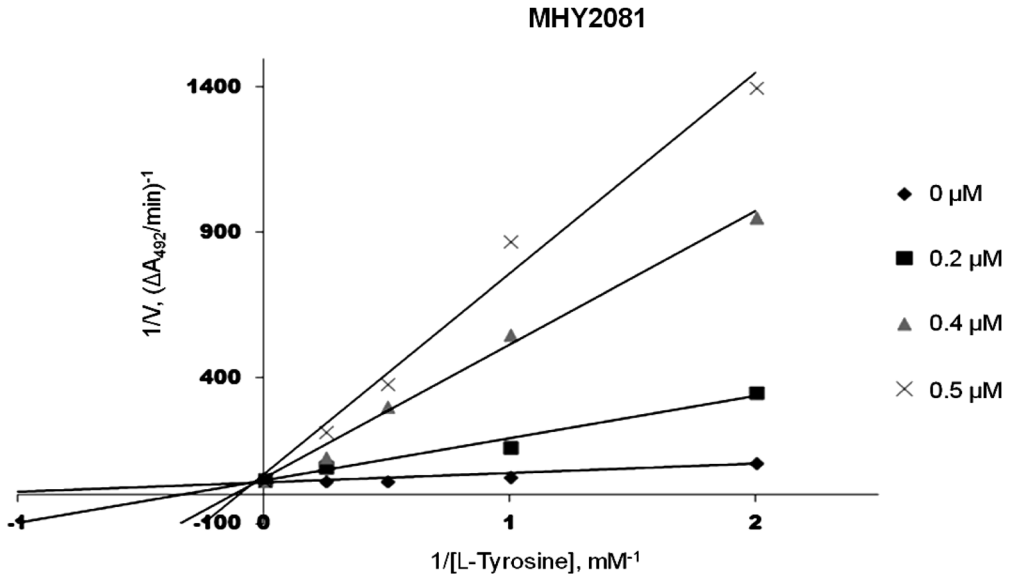

Fig. 3. MHY2081 Is a Competitive Inhibitor of Tyrosinase

Lineweaver–Burk plot of MHY2081 on mushroom tyrosinase. Data were obtained as mean values of 1/*V*, inverse of the increase of absorbance at a wavelength 492 nm per min, of three independent tests with different concentrations of L-tyrosine as a substrate.

lowed to grow to 70–80% confluence. Cells were incubated with kojic acid or MHY2081 for 2 h before α-MSH treatment. After MSH was treated, cells were incubated for 48 h. The cells were washed twice with phosphate buffered saline (PBS), detached by trypsin/ethylenediaminetetraacetic acid (EDTA), and dissolved in 80 μL of 1 N sodium hydroxide (NaOH) solution including 5% DMSO. The samples were incubated at 60°C for 1 h and mixed to solubilize melanin. Melanin concentration was analyzed by measuring absorbance at 405 nm.

Statistical Analysis All results are expressed as mean±standard error of the mean (S.E.M.). Treatments were compared using one-way ANOVA followed by Bonferroni test. A p values <0.05 were considered statistically significant.

RESULTS AND DISCUSSION

To screen for effective tyrosinase inhibitors, we synthesized (*Z*)-2-(benzo[*d*]thiazol-2-ylamino)-5-(substituted benzylidene)-thiazol-4(5*H*)-one derivatives based on the structure of well-known tyrosinase substrates L-tyrosine and L-DOPA (Table 1, Supplementary Fig. 1). *In vitro* tyrosinase activity assay using mushroom tyrosinase was performed to screen for the strongest tyrosinase inhibitor among thirteen derivatives. As shown in Table 1, introduction of two methoxy substituent at R^3 and R^5 positions on the phenyl ring of compound **1** (MHY 1887) increased tyrosinase inhibition 4-fold (33% inhibition) compared to compound **1** (8.6% inhibition) (Table 1). Surprisingly, introduction of a hydroxyl substituent at R^2 position on the phenyl ring of compound **1** increased tyrosinase inhibition by 11-fold (97% inhibition, MHY2081) while introduction of a hydroxyl substituent at R^3 position did not affect tyrosinase activity (Table 1). Introductions of hydroxyl, methoxy, ethoxy, or bromo substituent at other positions or/and replacement of the 4-hydroxyl group by a methoxy group on the phenyl ring of compound **1** did not affect tyrosinase activity (Table 1). Therefore, we focused on MHY2081 for further analysis. To further characterize the inhibitory effect of MHY2081 on tyrosinase, we examined dose-dependent inhibitory action of MHY2081 and calculated IC_{50} values. An *in vitro* tyrosinase activity assay using mushroom tyrosinase showed that MHY2081 efficiently inhibited tyrosinase activity with a dose-dependent manner. In addition, the inhibitory effect was greater than a well-known tyrosinase inhibitor kojic acid based on IC_{50} values (kojic acid=16.6 μM and MHY2081=1.8 μM) (Table 2), suggesting that MHY2081 efficiently blocks tyrosinase activity.

Because some well-known tyrosinase inhibitors including hydroquinone and kojic acids have cytotoxicity, we performed a MTT assay and confirmed that MHY2081 had no cytotoxicity up to 2 μM concentration in B16F10 melanoma cells (Fig. 1a). To further confirm whether MHY2081 inhibits intracellular tyrosinase function, we measured tyrosinase activity in B16F10 melanoma cells. A known tyrosinase activator α-MSH notably increased cellular tyrosinase activity (Fig. 1b). However, MHY2081 treatment significantly decreased cellular tyrosinase activity in α-MSH-treated melanoma cells with a dose-dependent manner (Fig. 1b). Tyrosinase is a key factor for melanin synthesis.[1)] To examine whether MHY2081-mediated inhibition of tyrosinase affects cellular melanin content, we measured melanin concentration in B16F10 melanoma cells. As expected, α-MSH increased cellular melanin concentration. However, MHY2081 treatment at 0.5 μM markedly reduced melanin content in α-MSH treated cells to the levels comparable to the control group without α-MSH treatment (Fig. 1c). Although MHY2081 at 1 and 2 μM further reduced melanin content, it was not dramatic. Therefore, MHY2081 at 0.5 μM may be enough for decreasing cellular melanin content.

Because MHY2081 was synthesized based on the structure of tyrosine with somewhat similarity, we examined whether MHY2081 directly binds to tyrosinase as an inhibitory mechanism using docking simulation. Docking simulation using AutoDock4.2 can calculate binding affinity between MHY2081 and tyrosinase. The structure images of tyrosinase from docking simulation showed that MHY2081 can directly bind to tyrosinase (Figs. 2a, b). Furthermore, binding energy for MHY2081 was greater than kojic acid (Fig. 2b), indicating that the binding affinity of MHY2081 to tyrosinase is greater

than that of kojic acid (tyrosinase docking score-kojic acid: −4.2 kcal/mol, MHY2081: −6.1 kcal/mol). To search for the binding residues of tyrosinase that correlated to kojic acid or new compound MHY2081, a LigandScout 3.1 program was applied. While kojic acid forms a hydrogen bond with a MET280 residue of tyrosinase and an aromatic interaction with HIS263, MHY2081 forms three hydrogen bonds with HIS61, HIS263, and ASN260 and a hydrophobic interaction with VAL283 (Figs. 2c, d), which contribute to higher affinity of MHY2081 to tyrosinase.

Based on docking simulation, we hypothesized that MHY2081 may competitively bind to tyrosinase with tyrosine. We analyzed the mode of inhibition of tyrosinase by Lineweaver–Burk plot analysis. As the concentrations of MHY2081 increased, K_m values gradually increased while V_{max} values were unchanged (Fig. 3), suggesting that MHY2081 is a competitive tyrosinase inhibitor.

In conclusion, MHY2081 competitively binds to tyrosinase with its substrate and inhibits tyrosinase activity without cytotoxicity, indicating that MHY2081 has an antimelanogenic effect. Therefore, MHY2081 is a novel compound for whitening cosmetics or treating pigmentation disorders.

Acknowledgments This work was supported by the National Research Foundation of Korea (NRF) Grant funded by the Korean government (MSIP) (Grant No. 2009-0083538) and Research Program through NRF funded by the Ministry of Education, Science and Technology (Grant No. NRF-2013R1A1A2009949). We thank Aging Tissue Bank for providing materials and research information.

Conflict of Interest The authors declare no conflict of interest.

Supplementary Materials The online version of this article contains supplementary materials.

REFERENCES

1) Brenner M, Hearing VJ. The protective role of melanin against UV damage in human skin. *Photochem. Photobiol.*, **84**, 539–549 (2008).
2) Khan MT. Novel tyrosinase inhibitors from natural resources—their computational studies. *Curr. Med. Chem.*, **19**, 2262–2272 (2012).
3) Liang C, Lim JH, Kim SH, Kim DS. Dioscin: a synergistic tyrosinase inhibitor from the roots of Smilax China. *Food Chem.*, **134**, 1146–1148 (2012).
4) Schallreuter KU, Kothari S, Chavan B, Spencer JD. Regulation of melanogenesis—controversies and new concepts. *Exp. Dermatol.*, **17**, 395–404 (2008).
5) Costin GE, Hearing VJ. Human skin pigmentation: melanocytes modulate skin color in response to stress. *FASEB J.*, **21**, 976–994 (2007).
6) Karioti A, Protopappa A, Megoulas N, Skaltsa H. Identification of tyrosinase inhibitors from *Marrubium velutinum* and *Marrubium cylleneum*. *Bioorg. Med. Chem.*, **15**, 2708–2714 (2007).
7) Satooka H, Kubo I. Resveratrol as a kcat type inhibitor for tyrosinase: potentiated melanogenesis inhibitor. *Bioorg. Med. Chem.*, **20**, 1090–1099 (2012).
8) Tocco G, Fais A, Meli G, Begala M, Podda G, Fadda MB, Corda M, Attanasi OA, Filippone P, Berretta S. PEG-immobilization of cardol and soluble polymer-supported synthesis of some cardol-coumarin derivatives: preliminary evaluation of their inhibitory activity on mushroom tyrosinase. *Bioorg. Med. Chem. Lett.*, **19**, 36–39 (2009).
9) Bilodeau ML, Greulich JD, Hullinger RL, Bertolotto C, Ballotti R, Andrisani OM. BMP-2 stimulates tyrosinase gene expression and melanogenesis in differentiated melanocytes. *Pigment Cell Res.*, **14**, 328–336 (2001).